Aerosol Science and Technology

ISSN: 0278-6826 (Print) 1521-7388 (Online) Journal homepage: http://www.tandfonline.com/loi/uast20

Emissions of Particulate Trace Elements, Metals and Organic Species from Gasoline, Diesel, and Biodiesel Passenger Vehicles and Their Relation to Oxidative Potential

K. L. Cheung , L. Ntziachristos , T. Tzamkiozis , J. J. Schauer , Z. Samaras , K. F. Moore & C. Sioutas

To cite this article: K. L. Cheung , L. Ntziachristos , T. Tzamkiozis , J. J. Schauer , Z. Samaras , K. F. Moore & C. Sioutas (2010) Emissions of Particulate Trace Elements, Metals and Organic Species from Gasoline, Diesel, and Biodiesel Passenger Vehicles and Their Relation to Oxidative Potential, Aerosol Science and Technology, 44:7, 500-513, DOI: 10.1080/02786821003758294

To link to this article: http://dx.doi.org/10.1080/02786821003758294

View supplementary material

Published online: 09 Jun 2010.

Submit your article to this journal

Article views: 1514

View related articles

Citing articles: 52 View citing articles

Full Terms & Conditions of access and use can be found at
http://www.tandfonline.com/action/journalInformation?journalCode=uast20

Download by: [University of North Texas] **Date:** 05 January 2017, At: 19:22

Aerosol Science and Technology, 44:500–513, 2010
Copyright © American Association for Aerosol Research
ISSN: 0278-6826 print / 1521-7388 online
DOI: 10.1080/02786821003758294

Emissions of Particulate Trace Elements, Metals and Organic Species from Gasoline, Diesel, and Biodiesel Passenger Vehicles and Their Relation to Oxidative Potential

K. L. Cheung,[1] L. Ntziachristos,[2] T. Tzamkiozis,[2] J. J. Schauer,[3] Z. Samaras,[2] K. F. Moore,[1] and C. Sioutas[1]

[1]*University of Southern California, Department of Civil and Environmental Engineering, Los Angeles, California, USA*
[2]*Laboratory of Applied Thermodynamics, Aristotle University, Thessaloniki, Greece*
[3]*University of Wisconsin, Department of Civil and Environmental Engineering, Madison, Wisconsin, USA*

Three light-duty passenger vehicles were tested in five configurations in a chassis dynamometer study to determine the chemical and oxidative potential of the particulate exhaust emissions. The first vehicle was a diesel Honda with a three-stage oxidation system. Its main catalyst was replaced with a diesel particulate filter (DPF) and tested as a second configuration. The second vehicle was a gasoline-fuelled Toyota Corolla with a three-way catalytic converter. The last vehicle was an older Volkswagen Golf, tested using petro-diesel in its original configuration, and biodiesel with an oxidation catalyst as an alternative configuration. Particulate matter (PM) was collected on filters and subsequently analyzed using various chemical and toxicological assays. The production of reactive oxygen species (ROS), quantified by the dithiothreitol (DTT) and macrophage-ROS assays, was used to measure the PM-induced oxidative potential. The results showed that the Golf vehicle in both configurations had the highest emissions of organic species (PAHs, hopanes, steranes, and organic acids). The DPF-equipped diesel Accord car emitted PM with the lowest amounts of organic species and the lowest oxidative potential. Correlation analyses showed that soluble Fe is strongly associated with particulate ROS activity (R = 0.99), while PAHs and hopanes were highly associated with DTT consumption rates (R = 0.94 and 0.91, respectively). In particular, tracers of lube oil emissions, namely Zn, P, Ca, and hopanes, were strongly correlated with distance-based DTT consumption rates (R = 0.96, 0.92, 0.83, and 0.91, respectively), suggesting that incomplete combustion of lube oil might be important driving factors of the overall PM-induced oxidative stress.

Received 24 August 2009; accepted 23 October 2009.
This work was funded by METRANS Center grant (MR-6068, USC account number 53-4507-6720), EPA PM Center grant (RD-8324-1301-0) and the Greek Secretariat for Research and Technology (Contract No 05NON-EU-137). We thank Mike Olson, Martin Shafer, and the staff at the Wisconsin State Laboratory of Hygiene for helping with the chemical measurements.
Address correspondence to C. Sioutas, University of Southern California, Department of Civil and Environmental Engineering, 3620 South Vermont Avenue, Los Angeles, CA 90089, USA. E-mail: sioutas@usc.edu

[Supplementary materials are available for this article. Go to the publisher's online edition of *Aerosol Science and Technology* to view the free supplementary files.]

1. INTRODUCTION

Motor vehicle emissions are the dominant sources of particulate matter (PM) in urban cities, and numerous studies have linked vehicular exhaust particles to adverse health effects, including premature deaths (Tsai et al. 2000; Hoek et al. 2002), respiratory and cardiovascular health problems (Stayner et al. 1998; Harrod et al. 2005; Pope and Dockery 2006; Seagrave et al. 2006; Gauderman et al. 2007; McDonald et al. 2007), and neurodegenerative disorders (Peters et al. 2006). Primary PM emitted by vehicles contains a variety of chemical constituents such as organic carbon, elemental carbon, trace elements, inorganic ions, etc. Its composition varies depending on the vehicle age and type, fuel, and after-treatment technology. Diesel particulate matter (DPM), in particular, is found to be harmful to both human health and the environment (Stayner et al. 1998; Lloyd and Cackette 2001). Both regulatory and engine manufacturing communities have devoted significant resources to emission reductions from diesel-powered engines.

To protect public health, more stringent PM mass based emission standards (US EPA 2007, 2010; EURO 4, 5) were promulgated. The new light-duty diesel vehicles introduced in the U.S. with the 2009 model year are equipped with after-treatment devices to meet the US EPA 2007 standards. With the exception of diesel vehicles operating with no emission control technologies, a substantial amount of PM emitted by both light- and heavy-duty vehicles is semi-volatile in nature, formed by condensation of super saturated vapors as they cool down in the ambient atmosphere (Sakurai et al. 2003; Biswas et al. 2009a). The semi-volatile PM fraction of vehicle emissions is extremely important in terms of its contribution to human exposure. Diesel particle filter technologies appear to remove the non-volatile fraction efficiently, but are less effective in controlling the volatile/semi-volatile portion (Biswas et al. 2009a). While numerous studies

have focused on the effects of different control technologies on emissions from heavy-duty diesel trucks, there is a limited number of papers in the literature discussing the composition of unregulated pollutants emitted from light duty diesel vehicles equipped with after-treatment devices. This information is vital in evaluating the overall effectiveness of after-treatment technologies in reducing emissions of harmful compounds to the atmosphere.

Within the last two decades, significant research on alternative motor vehicle fuels to address the adverse environmental effects (including climate change) of traditional fuels was undertaken. Among these, biofuels (which are virtually free of sulfur and aromatic compounds), are the focus of CO_2 abatement strategies due to their renewable character and their ability to be used in standard engines without modifications. Extensive research has been conducted to investigate the emissions of regulated species (Wang et al. 2000; Shi et al. 2006) from vehicles operating with biodiesel. However, there is a lack of toxicological data and detailed chemical analysis of unregulated species. It is therefore important to assess the toxic properties of PM emitted by vehicles using this type of fuel whose use is expected to be widespread in the future.

In this study, three light-duty vehicles in five different configurations (varying in vehicle type and age, fuel, and emission control technologies) were tested to study both the toxic activity of the emitted PM and the relevant factors affecting toxicity. The production of reactive oxygen species (ROS) has been shown to generate oxidative stress and play a direct role in modulating adverse health outcomes related to particle exposure (Donaldson et al. 2001; Li et al. 2003; Sheesley et al. 2003), and is therefore used to assess toxicity. Both molecular (dithiothreitol) and cellular (macrophage-ROS) assays are available to quantify the production of ROS. While these two assays are based on different biological mechanisms and pathways (see the Materials and Methods section for details), they nonetheless provide useful insights to the potential formation of ROS from particulate exhaust emissions. The objectives of this research were to collect samples from vehicles with distinctively different PM chemical profiles and identify the correlations between the chemical species and oxidative potential. This analysis will enable us to gain insight on the toxicological impacts of future changes in vehicle fleet and planned emission control strategies.

2. MATERIALS AND METHODS

2.1. Study Design

The chassis dynamometer experiments were carried out at the light-duty dynamometer facility of the Laboratory of Applied Thermodynamics at Aristotle University in Thessaloniki, Greece. A summary of the study design is described below, and further, more detailed information is provided in a previous study publication (Cheung et al. 2009).

Three light-duty passenger vehicles in five different configurations were tested. The first vehicle was a Honda Accord 2.2 L operated with low sulfur diesel (<10 ppm) fuel. This vehicle (Accord diesel) was equipped with a three-stage oxidation system including a closed-coupled oxidation catalyst, exhaust gas recirculation, and a main underbody oxidation catalyst, meeting the "Euro 4" emission standards. The main oxidation catalyst was then replaced with a diesel particulate filter (DPF) and tested as an alternative configuration (DPF-Accord). The DPF was a Pt-coated SiC filter of octagonal channel cross-section with 300 cells per square inch. The platinum coating acts as a media for catalytic oxidation. In this configuration, the vehicle complies with the expected (2010) "Euro 5" emission standards with regard to its PM emission levels. This car is considered representative of diesel emission levels of today and future vehicle technologies. The second vehicle was a "Euro 3"-compliant Toyota Corolla 1.8 L operated using unleaded gasoline with a research octane number of 95 and a nominal sulfur content of 50 ppm by weight. It was equipped with a typical three-way catalytic converter and twin lambda sensors. This gasoline vehicle (Corolla gasoline) was chosen to compare the oxidative potential between diesel and gasoline emissions, although the latter is known to have comparatively lower PM emission levels. The last vehicle was a Volkswagen Golf 1.9 L diesel passenger car, operated using diesel fuel with 50 ppm sulfur content. The originally equipped oxidation catalyst was removed to represent the baseline conditions (Golf diesel). It was therefore only a "Euro 1" vehicle with no after-treatment devices. The same vehicle was tested using sulfur-free neat soy biodiesel fuel (Golf biodiesel). When tested with the biodiesel, the vehicle was equipped with an oxidation catalyst, thus representing "Euro 2" compliance. Properties of the fuel (both petro-diesel and biodiesel) used in the Golf vehicle are listed in Table 1. A tabulated comparison of the 5 configurations in this study can be found in Table S1 of Cheung et al. (2009). All vehicles are owned by the Laboratory of Applied Thermodynamics and the manufacturer's maintenance schedule has been followed for each. All after-treatment devices (except (removal of) the DPF) have been used over the lifetime of the vehicles tested (45,000 km for the Honda Accord, 100,000 km for the Toyota Corolla, and 168,000 km for the Volkswagen Golf). It should also be noted that the addition or removal of a control device might lead to changes in the engine operation, and the exhaust emissions in this study were not optimized with the configurations used. The emission rates might be different if the engine and the after-treatment system is calibrated and optimized in the new configuration.

Each vehicle/configuration was driven on the chassis dynamometer using the same protocol: a variety of real-world driving cycles (Artemis Cycles) (Andre 2004) and the certification test (New European Driving Cycle). The three Artemis driving cycles (urban, rural road, and motorway) consist of frequent speed variation and stronger acceleration compared to the NEDC, and were designed to simulate typical driving conditions in Europe. The vehicle and the sampling system were pre-conditioned by running three extra urban driving cycles (EUDC), according to the specifications of the UNECE R83 regulation. After the pre-conditioning, the vehicle was conditioned at room temperature for at least 8 hours before conducting the

TABLE 1
(a) Fuel properties of the petrodiesel used in the Golf vehicle

Properties	Units	Petroleum diesel	EN 590 limits	Test method
Viscosity (40°C)	$mm^2\ s^{-1}$	3.61	2.00–4.50	EN ISO 3104
Density (15°C)	$g\ cm^{-3}$	0.8345	0.820–0.845	EN ISO 3675
Flash point	°C	71	55 min	EN 22719
Sulfur content	$\mu g\ g^{-1}$	29	50 max	EN ISO 20846
Water content	$\mu g\ g^{-1}$	52	200 max	EN ISO 12937
Cold filter plugging point (CFPP)	°C	–9	+ 5 max	EN 116
Cetane number		55.5	51 min	EN ISO 5165
Distillation				EN ISO 3405
Initial boiling point (IBP)		179		
10%		220		
50%		281		
90%		344		
Final boiling point (FBP)		367		
Gross heating value	$cal\ g^{-1}$	10900	—	IP 12

(b) Fuel properties of the biodiesel used in the Golf vehicle

Property	Units	Biodiesel	EN 14214 limits	Test method
Viscosity, 40°C	$mm^2\ s^{-1}$	4.4	3.5–5.0	EN ISO 3104
Density, 15°C	$g\ cm^{-3}$	0.8816	0.860–0.900	EN ISO 12185
Flash point	°C	>166	120 min	EN ISO 3679
Sulfur content	$\mu g\ g^{-1}$	2.0	10.0 max	EN ISO 20846
Water content	$\mu g\ g^{-1}$	450	500 max	EN ISO 12937
Copper strip corrosion (3 h at 50°C)	Rating	1A	Class 1	EN ISO 2160
CFPP	°C	–7	–5 max	EN 116
Cetane number		52	51 min	EN ISO 5165
Sulfated ash content	%(m/m)	<0.01	0.02 max	ISO 3987
Oxidation stability, 110°C	Hours	4.6	6 min	EN 14112
Iodine number		122	120 max	EN 14111
Acid value	$mg\ KOH\ g^{-1}$	0.4	0.50 max	EN 14104
Monoglyceride content	%(m/m)	0.77	0.80 max	EN 14105
Diglyceride content	%(m/m)	0.19	0.20 max	EN 14105
Triglyceride content	%(m/m)	0.11	0.20 max	EN 14105
Free glycerol	%(m/m)	0.05	0.02 max	EN 14106
Total glycerol	%(m/m)	0.23	0.25 max	EN 14105
Methanol content	%(m/m)	0.12	0.20 max	EN 14110
Ester content	%(m/m)	96.6	96.5 min	
Linolenic acid methyl ester	%(m/m)	5.77	12 max	
Group I Metals (Na+K)	$\mu g\ g^{-1}$	<0.01, 0.9	5.0 max	EN 14108 EN 14109
Phosphorous content	$\mu g\ g^{-1}$	5	10 max	EN 14107
Gross heating value	$cal\ g^{-1}$	9228	—	IP 12

tests, in order to effectively achieve a cold-start in the next sampling period. In the case of the DPF-equipped car, the filter was regenerated before installation on the vehicle and a moderate soot loading was accumulated over the three EUDCs used for pre-conditioning. Monitoring of the inlet and outlet temperature in the filter ensured that no regeneration occurred during our measurements.

The exhaust gas was primarily diluted and conditioned in a dilution tunnel, following the regulated constant volume sampling (CVS) technique. A 6 m long corrugated stainless steel

tube transferred the exhaust from the tailpipe to the CVS dilution tunnel inlet. The tube was insulated to minimize heat losses and particle thermophoresis and was clamped onto the vehicle exhaust pipe with a metal-to-metal connection to avoid exposing the hot exhaust gas to any synthetic material connectors. The CVS flow rate was maintained constantly at 600 Nm^3/h by a positive displacement pump. PM from the CVS tunnel was collected by filters. Tunnel filter blanks were also collected to measure the background concentration of the dilution tunnel. The sampling system consisted of two filter holders hosting Quartz (47 mm Pallflex TISSU Quartz 2500 QAT-UP) and polytetrafluoroethylene (Teflon – 47 mm Pallflex TX40HI20-WW) filters, a Versatile Aerosol Concentration Enrichment System (VACES) (Kim et al. 2001; Zhao et al. 2005) and two additional Quartz and Teflon filters downstream of the VACES. (Figure 1, Cheung et al. 2009 for a schematic of the sampling setup.) In this article, only the results from the Quartz filter collected upstream of the VACES are discussed in details (the results using the VACES are reported by Cheung et al. 2009). The nominal flow rates through the upstream filters were 20 lpm, and were recorded by TSI 4043 flow meters with a certified accuracy of 2%. After sampling, all filter samples were stored in the –20°C freezers until subsequent analysis.

2.2. Chemical Analysis

Total emitted PM mass concentrations have been determined by weighing the Teflon filter substrates used to collect the exhaust emissions. Water extracts of the Teflon filters were analyzed for water soluble organic carbon (WSOC) and inorganic ions, using a Sievers Total Organic Carbon analyzer (General Electric, Inc.) (Zhang et al. 2008) and ion chromatography (Lough et al. 2005), respectively. Elemental carbon (EC) and organic carbon (OC) analyses were conducted using the Quartz filters according to the NIOSH Thermal Desorption/Optical Transmission method (Birch and Cary 1996). Detailed chemical analyses of mass, WSOC, IC, and EC/OC were presented in Cheung et al. (2009).

The analyses conducted below constitute the basis of this article. The Inductively Coupled Plasma-Mass Spectroscopy (ICP-MS) was used to determine the concentrations of the water soluble trace elements in the particles. The results from the ICP analysis include the following: Na, Mg, Al, K, Ca, Ti, V, Cr, Be, S, Mn, Fe, Co, Cu, Zn, Mo, V, Sr, Ba, Cd, Pt, Pb, and Ni. They were selected due to their toxic potential through inhalation (Vogl and Elstner 1989; Becker et al. 2005). Lough et al. (2005) describes the procedures for the sample processing (e.g., filter/substrate extraction methods and digestion). The organic species, including polycyclic aromatic hydrocarbon (PAHs), hopanes, steranes, n-alkanes, and organic acids, were quantified by gas chromatography/mass spectrometry (GC/MS) (Stone et al. 2008).

The toxic activity of exhaust emission was evaluated using a cellular ROS assay in addition to the molecular dithiothreitol (DTT) test. In brief, the DTT test provides a measure of the overall redox activity of the sample based on the ability to catalyze electron transfer between DTT and oxygen in a cell-free system (Cho et al. 2005). Details of this method were presented in Cheung et al. (2009). Cellular production of ROS by the emissions samples was measured using a rat alveolar macrophage assay. Details of the assay have been presented by Landreman et al. (2008) and are only briefly described here. Samples were extracted with purified water and then filtered with a 0.22 μm pore size filter to isolate the water-soluble and colloidal fraction of the sample. The sample extracts were then buffered in a salt and glucose medium and subsequently split to prepare aliquots of diluted and non-diluted samples for cell exposures in triplicate. The aliquots were mixed with NR8383 rat alveolar cells that were grown from samples obtained from the American Type Culture Collection (ATCC) and 2′7′-dicholorohidroflourescin diacetate (DCFH-DA) in 96-well plates and incubated at 37°C for 2 h. Fluorescence intensity after the incubation was measured using a Cytoflour II automated fluorescence plate reader. Positive and negative controls were analyzed along with each set of samples. Un-opsonized Zymosan (a β-1,3-polysachharide of D-glucose) was used as a primary positive control and all results were reported in units of Zymosan equivalents. This ROS assay has been previously used to characterize a wide range of aerosol samples including atmospheric particulate matter samples from Denver (Zhang et al. 2008) and Los Angeles (Hu et al. 2008), as well as atmospheric aerosol samples impacted by large forest fires (Verma et al. 2009).

The results presented in this article were tunnel blank subtracted to account for trace levels of individual chemical constituents in the sampling tunnel. Tunnel blank subtracted values ≤ 0 were reported as below detection limit (BDL), and were interpreted as zeros in all calculations and correlations. Tunnel blanks subtracted values that are larger than zero are reported with uncertainties. A limit of detection (LOD) table is provided in the online Supplemental Information as a reference; and the detection limit is defined as 3 times the analytical uncertainty in this study.

3. RESULTS AND DISCUSSION

3.1. Emission Factors of Trace Elements and Metals

Table 2 lists emission factors of: (a) PM mass, elemental carbon (EC), organic carbon (OC), and sulfate, (b) selected trace elements and metals. Crustal elements are shown at the top of the Table 2b because their contributions to elemental emissions are higher than anthropogenic elements in diesel vehicles (Wang et al. 2003). Emission factors in Table 2a were reported and discussed in detail in the previous publication (Cheung et al. 2009), and are only included here to put the rest of the results in perspective. In summary, the Golf diesel and biodiesel vehicles were characterized by the highest PM mass emissions. The DPF-equipped diesel vehicle reduced 98% of the mass emissions compared to its original configuration, and to a level lower than the gasoline car.

Sulfur emissions were highest among the non-metallic elements in each vehicle/configuration. The high sulfur emission

TABLE 2
(a) Emission factors of PM mass (mg/km), elemental carbon (mg/km), organic carbon (mg/km), and sulfate (mg/km).
(b) Emission factors of selected trace elements and metals (ng/km)

	Accord diesel	DPF-Accord	Corolla gasoline	Golf diesel	Golf biodiesel
a					
PM Mass*	27.13	0.63	2.41	72.08	41.20
Elemental carbon*	19.6 ± 0.5	0.03 ± 0.01	0.05 ± 0.01	39.1 ± 1.08	6.73 ± 0.19
Organic carbon*	4.92 ± 0.14	0.51 ± 0.03	0.95 ± 0.04	24.2 ± 0.6	24.4 ± 0.6
Sulfate*	0.07 ± 0.01	0.1 ± 0.01	0.99 ± 0.05	0.14 ± 0.01	0.26 ± 0.01
b					
Al	148 ± 43	20.6 ± 12.3	21.1 ± 12.8	1,160 ± 38	83.1 ± 27.2
Ca	15,100 ± 1,340	BDL	29,700 ± 742	118,000 ± 2,080	54,200 ± 1,740
Fe	5.23 ± 20.5	10.0 ± 8.6	622 ± 10	618 ± 17	428 ± 19
Mg	5,100 ± 127	260 ± 45	1,590 ± 69	4,740 ± 140	8,200 ± 176
Na	17,700 ± 566	BDL	4,760 ± 160	25,300 ± 356	149,000 ± 2,650
P	4,590 ± 148	254 ± 49	3,670 ± 56	31,800 ± 682	29,900 ± 604
S	24,500 ± 1,460	30,800 ± 1,170	301,000 ± 6,350	81,400 ± 1,660	78,000 ± 1,130
K	10,300 ± 581	BDL	4,050 ± 298	13,500 ± 953	524,000 ± 28,600
V	37.8 ± 2.9	BDL	5.26 ± 0.84	27.3 ± 1.6	47.2 ± 2.1
Cr	341 ± 7	67.6 ± 4.6	46.4 ± 6.5	245 ± 7	247 ± 8
Mn	124 ± 24	35.3 ± 11.2	1,640 ± 16	426 ± 23	432 ± 23
Co	5.78 ± 0.70	2.85 ± 0.69	17.5 ± 0.5	23.2 ± 0.9	64.8 ± 1.8
Ni	160 ± 21	104 ± 10	158 ± 10	196 ± 21	59.2 ± 18.7
Cu	BDL	BDL	708 ± 8	BDL	46.3 ± 11.0
Zn	7,020 ± 164	372 ± 65	2,260 ± 60	22,300 ± 187	22,300 ± 403
Cd	5.23 ± 0.79	0.82 ± 0.28	2.69 ± 0.48	5.53 ± 0.88	4.08 ± 0.96
Ba	142 ± 26	BDL	42.1 ± 10.0	185 ± 21	199 ± 19
Pb	18.2 ± 0.8	2.39 ± 0.35	27.9 ± 0.4	247 ± 2	14.1 ± 0.7

*Data reported in Table 1, Cheung et al. (2009).

observed in the gasoline vehicle is consistent with the inorganic ions data, which showed high sulfate ion emissions. Sulfate emission (0.99 mg/km) was about 3.2 times that of sulfur (0.30 mg/km), very close to the molecular weight ratio of sulfate to sulfur, suggesting that most of the sulfur come from sulfates. When compared with the Golf diesel vehicle, which used fuel with the same sulfur content and lube oil with different sulfur content, the gasoline car yielded higher sulfur emissions. The diesel vehicle used a lubrication oil of 8900 ppm S, while the respective value for the oil used in the gasoline vehicle was 5000 ppm. Since our historical records of lubricant oil consumption rates for the two vehicles (∼50 ml/1000 km) do not provide evidence of higher consumption of the gasoline than the diesel vehicle, we hypothesize that the high sulfate emissions in the gasoline car are due to the formation of sulfate nanoparticles through nucleation processes occurring downstream of the 3-way catalytic converter. Gasoline vehicles do not usually produce high sulfate levels because there is no oxygen surplus in the exhaust to oxidize sulfur. This particular gasoline vehicle, however, was equipped with secondary air injection, i.e., a small quantity of secondary air (SAI) is injected into the exhaust when required to oxidize hydrocarbons and carbon monoxide. This SAI may result in high sulfate formation as it provides the missing oxygen to form sulfates. The gasoline vehicle was also characterized by higher emissions of Mn, Fe, and Cu compared with the DPF-Accord vehicle, consistent with previous studies (Geller et al. 2006). Mn is a known knock improver; it was probably used in the gasoline car at trace concentration levels in order to improve the octane number of the fuel.

Despite the high emission reductions of most inorganic ions, the Accord vehicle shows a 26% increase in sulfur emissions when equipped with the DPF. Several earlier studies showed that particle nucleation in diesel vehicles occurs following the after-treatment devices (Vaaraslahti et al. 2004; Kittelson et al. 2006; Biswas et al. 2009b). For example, Vaaraslahti et al. showed formation of new particles occurred downstream of the DPF and suggested that sulfuric acid was the main nucleating species (Vaaraslahti et al. 2004). Biswas et al. (2009b) showed that the formation of fresh nanoparticles via nucleation in DPF-equipped diesel trucks was attributed to a ternary nucleation process involving sulfuric acid, water vapor, and ammonia. These observations are consistent with our study.

Sulfur emissions are similar between the two configurations (petro-diesel or biodiesel) of Golf vehicle, which used the same

lube oil, suggesting that a significant fraction of sulfur in these configurations may be originating from lube oil. The diesel vehicle (Golf) used a fuel with a 50 ppm S content, and without any after-treatment technology, particulate sulfur could be contributed by both the fuel and the lube oil. But its sulfur emission (81.4 μg/km) is relatively low considering the high sulfur content in its fuel. Thus, it is believed that most of the sulfur was converted to SO_2 and released as a gas. Although the biodiesel vehicle had less sulfur in its fuel, its oxidation catalyst may counterbalance the reduced sulfur by oxidizing any trace sulfur in the fuel and the lube oil.

Potassium and sodium emissions were higher in the biodiesel vehicle compared to the same vehicle operating with diesel by factors of 39 and 6, respectively. The increased emissions of these species may be due to the fact that KOH and NaOH were used as catalysts in the esterification process. These compounds probably remained in the biodiesel and were subsequently emitted as particles.

3.2. Emission Factors of Organic Species

Table 3 shows the emission factors of PAHs, hopanes, steranes, alkanes, and organic acids (OA). PAHs are subdivided into three categories according to their molecular weights (MW): MW $\leq$ 228 [Phenanthrene, anthracene, fluoranthene, acephenanthrylene, pyrene, methylfluoranthene, benzo(GHI)-fluoranthene, cyclopenta(cd)pyrene, benz(a)anthracene, chrysene], MW = 252 [Benzo(b)fluoranthene, benzo(k)-fluoranthene, benzo(j)fluoranthene, benzo(e)pyrene and benzo(a)pyrene] and MW $\geq$ 276 [Indeno (1,2,3-cd)pyrene, benzo(ghi)perylene, dibenz(ah)anthracene, picene, coronene, and dibenzo(ae)pyrene]. Unsurprisingly, the Golf diesel vehicle with no after-treatment device emitted the highest amount of PAHs, followed by the biodiesel car. The gasoline vehicle emitted higher proportions of heavy PAHs (MW $\geq$ 276) compared to the petro-diesel vehicles, also consistent with previous studies (Miguel et al. 1998; Zielinska et al. 2004). Heavier MW PAHs are emitted only from the gasoline and biodiesel cars. Light MW PAH (MW $\leq$ 228) emissions were highest for the Golf diesel vehicle, followed by the Golf biodiesel and the Accord diesel. Biodiesel emissions of light MW PAHs were modestly reduced by 50% compared with its original (diesel) configuration, as previously reported (Correa and Arbilla 2006; Chien et al. 2009). This reduction could be attributable to the properties of the soybean biodiesel. Unlike petro-diesel, this fuel has very little or negligible aromatic content. The oxygen atoms in the biodiesel esters together with the oxidation catalyst might have also facilitated the oxidation of the PAHs. The different PAH profile of the biodiesel vehicle compared to its diesel configuration also provides a good indication of the distinct combustion chemistry between biodiesel and petro-diesel. Biodiesel contains unsaturated components and results in higher flame temperatures than petro-diesel, providing favorable conditions for the formation of larger PAH molecules (Jha et al. 2008).

Light MW PAHs are important in terms of the potential to generate oxidative stress (Li et al. 2003). While heavier MW PAHs are typically present in the particle phase, the light MW semi-volatile PAHs partition between the gas and particle phases. The Accord with the DPF removed the semi-volatile PAHs to levels below their detection limits, which is much lower than emissions from the Accord in its original configuration, highlighting its effectiveness from the toxicological perspective. The Golf diesel vehicle emitted the highest amounts of semi-volatile PAHs compared with the other two vehicles. As stated earlier, the semi-volatile PAHs emissions of the biodiesel vehicle was decreased by 50%, compared to its baseline petro-diesel configuration. Nonetheless, the sum of the semi-volatile PAHs from the biodiesel car (7.76 μg/km) is still much higher than the Accord diesel (2.55 μg/km), the DPF-Accord (BDL) and the gasoline vehicles (0.20 μg/km).

Figure 1 shows 12 of the 16 U.S. EPA priority PAHs identified in this study of which 7 are probable human carcinogens. The baseline diesel vehicle emitted the highest total sum of these 12 PAHs (13.9 μg/km), followed by biodiesel (8.54 μg/km) and the Accord diesel (2.55 μg/km). The DPF-equipped Accord diesel vehicle removed the 12 PAHs to levels below their

TABLE 3
Emission factors (μg/km) of PAHs, hopanes, steranes, alkanes, and organic acid (OA)

	Accord diesel	DPF-Accord	Corolla gasoline	Golf diesel	Golf biodiesel
Σ PAHs	2.55 ± 0.43	BDL	0.67 ± 0.08	16.5 ± 1.4	10.4 ± 0.9
Σ PAHs, MW ≤ 228	2.25 ± 0.43	BDL	0.20 ± 0.05	15.6 ± 1.4	7.76 ± 0.90
Σ PAHs, MW = 252	BDL	BDL	0.22 ± 0.04	0.90 ± 0.16	1.34 ± 0.19
Σ PAHs, MW ≥ 276	BDL	BDL	0.25 ± 0.04	BDL	1.34 ± 0.2
Σ Hopanes	0.94 ± 0.15	0.01 ± 0.02	0.09 ± 0.03	67.9 ± 5.5	59.5 ± 4.8
Σ Steranes	BDL	BDL	BDL	23 ± 1.9	20.2 ± 1.6
Σ Alkanes	197 ± 30	6.95 ± 5.34	9.78 ± 3.09	981 ± 84	125 ± 27
Σ Organics acids	1.04 ± 3.74	6.67 ± 4.84	7.13 ± 4.95	342 ± 43	5,240 ± 355
Σ OA, C9-14	BDL	1.32 ± 1.12	1.71 ± 1.33	11.3 ± 5.0	17.7 ± 6.3
Σ OA, C15-29	1.04 ± 3.74	5.35 ± 4.70	5.42 ± 4.77	331 ± 43	5,220 ± 354

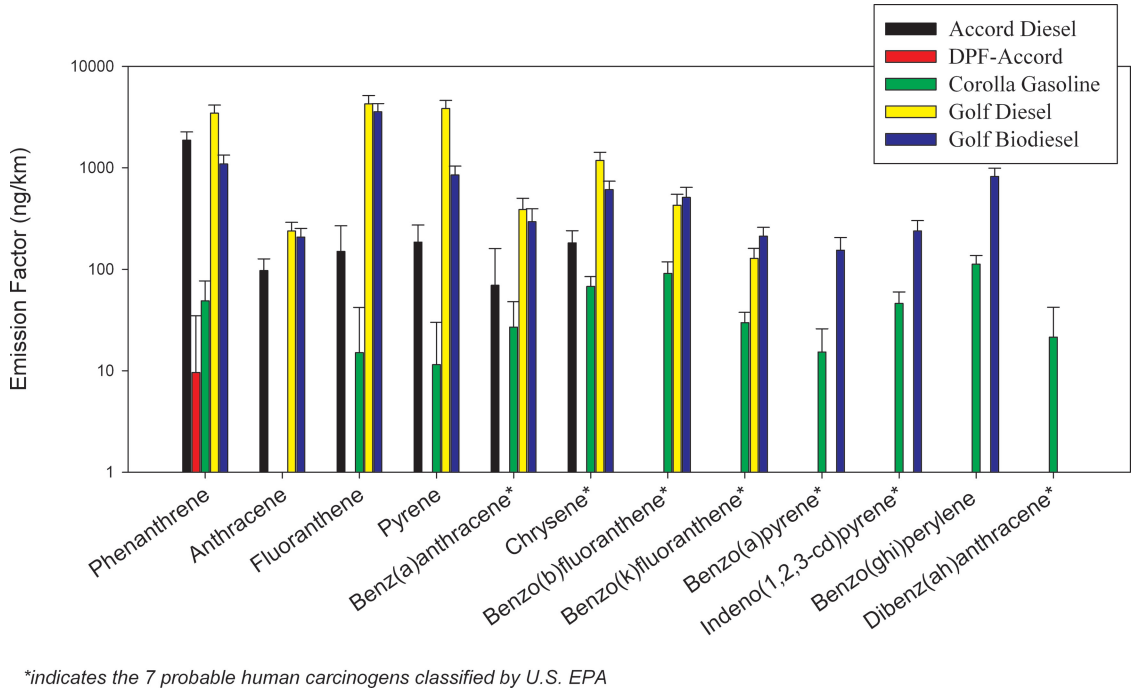

FIG. 1. Emission factors (ng/km) of 12 priority polycyclic aromatic hydrocarbons (PAHs) classified by the US EPA.

detection limits as a result of the effectiveness of the DPF in removing these carcinogenic compounds. The Golf diesel vehicle emitted 4 out of the 7 probable carcinogenic PAHs, ranging from 128 to 1180 ng/km. The same vehicle operated using biodiesel emitted 6 out of 7 probable carcinogenic PAHs at concentrations varying from 154 to 609 ng/km. The gasoline car emitted a considerable amount of carcinogenic PAHs, but in concentrations lower than the baseline diesel and biodiesel vehicles. Our findings therefore indicate that the use of efficient emission control technologies (such as DPF) or cleaner fuel (gasoline) may be far more effective in reducing the emissions of carcinogenic substances like PAHs than the use of biodiesel.

Figure 2 shows the emission factors of individual hopanes and steranes. Hopanes and steranes originate from lube oil and are widely used as tracers of vehicular emissions (Rogge et al. 1993; Fraser et al. 1999). The Golf vehicle emitted the highest hopane and sterane emissions in both of its configurations compared with the other two vehicles. Although the biodiesel configuration was equipped with an oxidation catalyst, it did not effectively remove any hopanes and steranes. In addition, the obvious similarity in the emission factors and profiles of hopanes and steranes suggests that they were exclusively from lube oil, since these two vehicle configurations used different fuel (petro-diesel and biodiesel) but the same lube oil. When the emission factors (μg/km) of the hopanes are normalized to total carbon (OC+EC) (mg/km), the ratios are 1073 and 1911 μg/g for the Golf diesel and Golf biodiesel vehicles, respectively. The difference might be attributable to the much lower EC levels in the biodiesel configuration. The DPF-Accord vehicle, on the other hand, yielded high reductions of hopanes and steranes compared to its original configuration. The DPF reduced 4 of the 7 hopanes to concentration levels below their limits of detection. The Accord diesel and the gasoline vehicle did not emit detectable amounts of steranes. This may be important in future studies. As steranes are often used as tracers of vehicle exhaust, non-detectable emissions by cleaner and newer vehicles might impact modeling efforts in source apportionment studies.

Alkanes are species that may originate from diesel fuel as well as unburned oil. Thus, high alkane emissions are observed for the baseline diesel vehicle, followed by the Accord diesel vehicle. Figure 3 shows the emission factors of speciated alkanes for each vehicle/configuration. The Golf diesel vehicle with no after-treatment technology emitted high levels of nonadecane, eicosane, heneicosane, and docosane (ranging from 139 to 215 μg/km). The newer Accord diesel vehicle had overall lower alkane emissions, but emitted a more diverse profile of these species than the Golf vehicle. In contrast, alkane levels were low in the biodiesel vehicle since this type of biodiesel (B100) does not contain alkanes. This is important in terms of source apportionment modeling in fleets with a high proportion of biodiesel vehicles.

Figure 4 shows the emission factors of organic acids detected in our study. Hexadecanoic acid, octadecanoic acid, oleic acid, linoleic acid, and linolenic acid are ingredients of soybean biodiesel (Kincs 1985). High emissions of hexadecanoic acid, octadecanoic acid, oleic acid, and linoleic acid are observed in the biodiesel vehicle, consistent with the reported components. Linolenic acid was not detectable in this vehicle's emissions

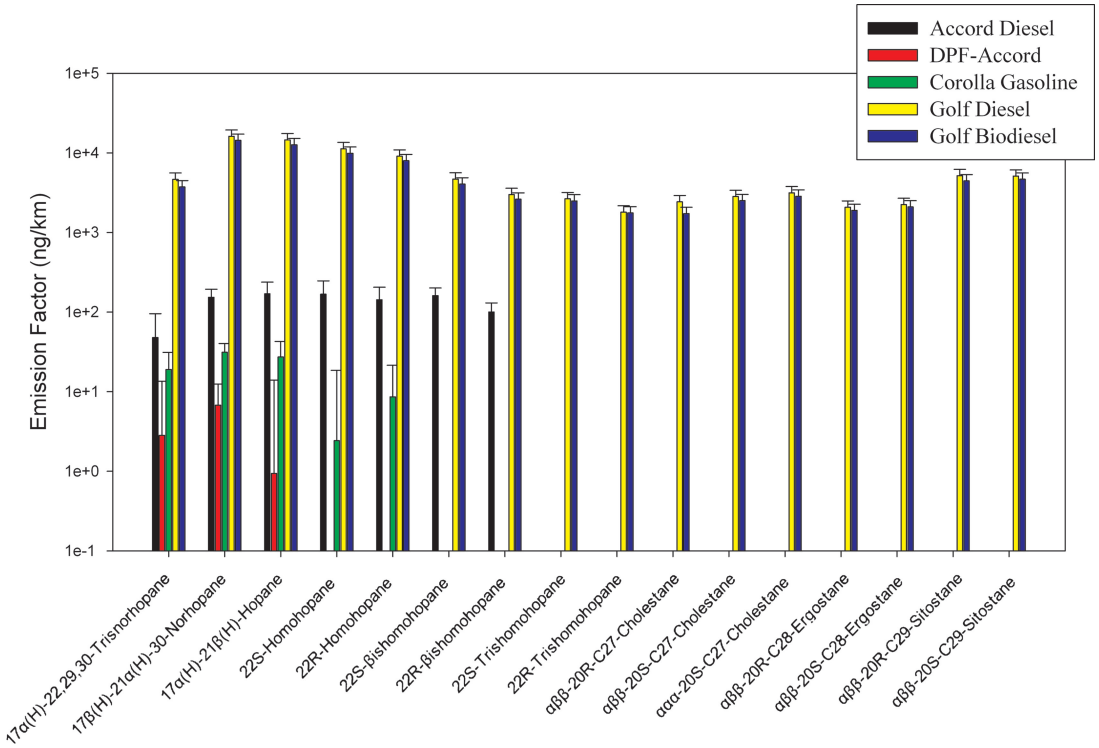

FIG. 2. Emission factors (ng/km) of hopanes and steranes.

probably because it is an unstable compound with three double bonds, in contrast to the other acids, which are much more stable. The biodiesel fuel used in the study is composed of methyl esters produced from soybeans. During the combustion process, these methyl esters may demethylate at high temperatures (Knothe 2006). In particular, the biodiesel used in this study had a low stability due to its high linolenic acid ester (5.8%) content. Since the analyses of the fatty acids were done by converting these acids to methyl esters, the high emissions of these acids are expected to originate from the esters, as well as the acids formed during demethylation. The high emissions of organic acids and/or esters are a result of incomplete combustion of biodiesel fuel, which is also consistent with the higher PM mass emissions from the biodiesel.

As described earlier, the DPF employed in this study was a platinum coated silicon carbide filter of octagonal channel

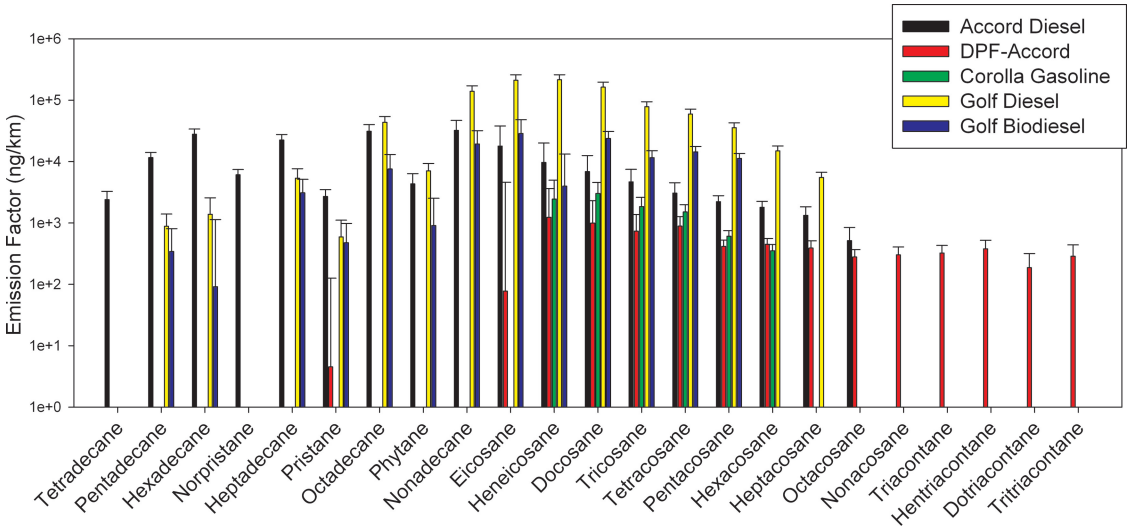

FIG. 3. Emission factors (ng/km) of selected n-alkanes.

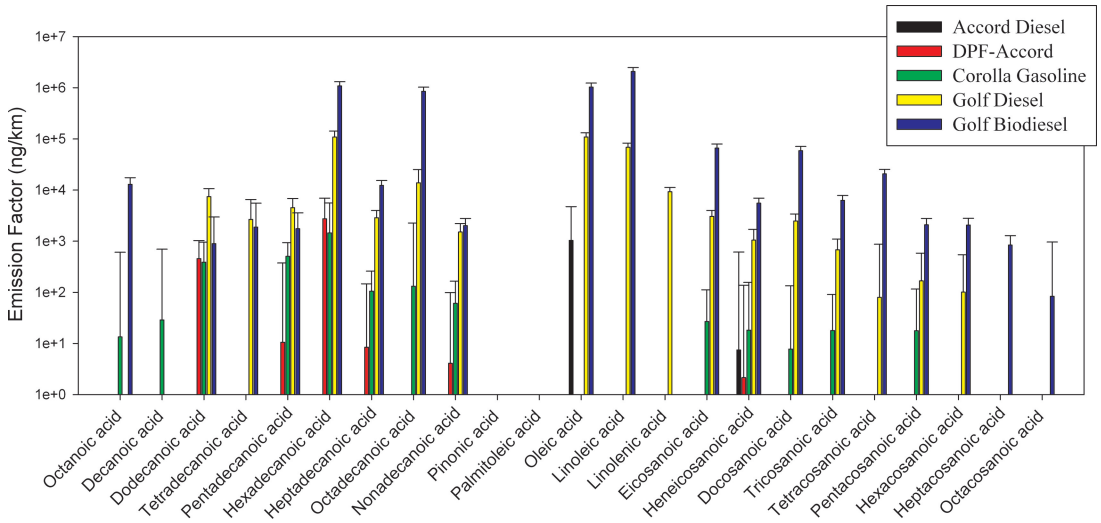

FIG. 4. Emission factors (ng/km) of selected organic acids.

cross-section with a cell density of 300 cells/in^2. Figure 5 shows the DPF removal rates of selected elements, PAHs, elemental carbon, organic carbon and water soluble organic carbon, (for the Accord vehicle, S and Fe are not included in the figure since they were elevated in the DPF configuration). Elevated sulfur concentrations were probably due to nucleation following the filter as discussed earlier. Fe, on the other hand, was present in trace levels with high uncertainties. Cu is excluded due to the low levels observed and the associated uncertainties. Overall, Figure 5 shows lower removal efficiency for certain elements (35, 51, 71, and 80% for Ni, Co, Mn, and Cr, respectively). Part of this lower removal efficiency may be due to analytical uncertainties associated with the already low emission levels of some of these trace elements.

The DPF removed much higher relative amounts of PAHs than trace elements. All PAHs originally present in the Accord vehicle were removed to levels below detection limits. Meanwhile, only 90% of the organic carbon was removed. Since the DPF in the Accord vehicle also acted as a catalyst, the differential removal efficiency for OC and the PAHs might be

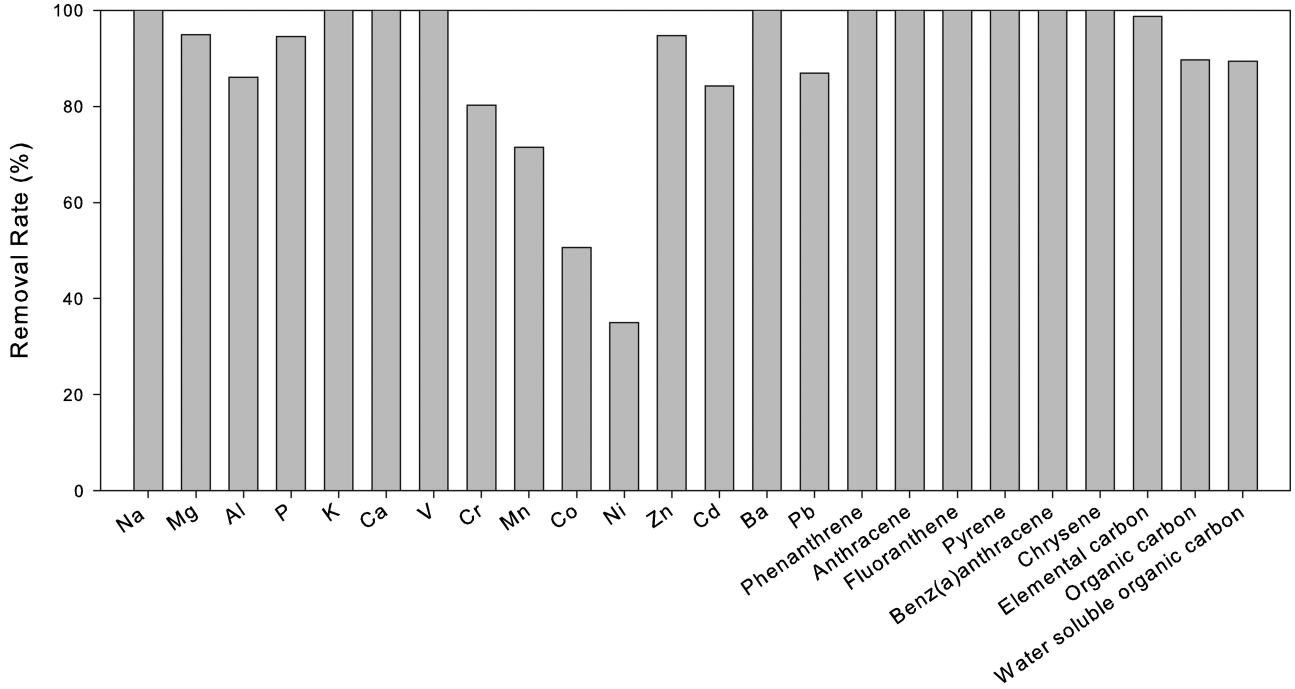

FIG. 5. DPF removal rates (%) of selected trace elements and metals, selected PAHs, elemental carbon, organic carbon, and water soluble organic carbon of the Honda Accord vehicle.

TABLE 4

Correlations coefficients, R, among selected PM chemical constituents

	Mg	Al	P	S	K	Ca	V	Cr	Mn	Fe	Co	Ni	Zn	Cd	Ba	Pb	ΣPAHs	ΣPAHs, MW ≤ 228	ΣPAHs, MW = 252	Σ Hopanes	Σ Alkanes	Σ Organic acids	Σ OA, C9–14	Σ OA, C15–29
Na	0.84	−0.10	0.68	−0.17	**0.99**	0.26	0.75	0.38	−0.12	0.21	**0.96**	−0.70	0.71	0.27	0.67	−0.13	0.46	0.35	0.85	0.64	−0.05	**0.99**	0.87	**0.99**
Mg		0.21	0.76	−0.29	0.77	0.46	**0.98**	0.79	−0.22	0.20	0.79	−0.28	0.84	0.73	**0.94**	0.15	0.64	0.57	0.77	0.70	0.28	0.77	0.77	0.77
Al			0.66	−0.16	−0.21	**0.90**	0.19	0.35	−0.14	0.47	0.02	0.64	0.63	0.61	0.52	**0.99**	0.84	**0.90**	0.39	0.69	**1.00**	−0.17	0.36	−0.17
P				−0.16	0.59	0.88	0.65	0.46	−0.11	0.58	0.76	−0.05	**0.99**	0.62	0.86	0.64	**0.96**	**0.92**	**0.94**	**0.99**	0.69	0.62	**0.93**	0.62
S					−0.13	0.04	−0.04	−0.59	**1.00**	0.69	0.06	0.22	−0.24	−0.18	−0.30	−0.04	−0.21	−0.23	−0.04	−0.19	−0.21	−0.13	−0.13	−0.13
K						0.15	0.66	0.27	−0.09	0.17	**0.95**	−0.78	0.61	0.14	0.56	−0.24	0.35	0.23	0.80	0.56	−0.17	**1.00**	0.82	**1.00**
Ca							0.37	0.33	0.07	0.72	0.41	0.41	0.84	0.66	0.70	**0.92**	**0.95**	**0.96**	0.71	**0.88**	**0.91**	0.19	0.66	0.19
V								**0.89**	−0.33	0.04	0.65	−0.21	0.76	0.78	**0.93**	0.11	0.56	0.51	0.64	0.59	0.27	0.66	0.63	0.66
Cr									−0.52	−0.19	0.24	0.12	0.59	0.86	0.83	0.25	0.50	0.50	0.31	0.41	0.43	0.27	0.32	0.27
Mn										0.72	0.11	0.23	−0.19	−0.11	−0.22	−0.02	−0.17	−0.19	0.01	−0.15	−0.18	−0.09	−0.09	−0.09
Fe											0.47	0.28	0.49	0.29	0.32	0.56	0.55	0.53	0.59	0.56	0.44	0.20	0.50	0.20
Co												−0.58	0.76	0.28	0.66	0.02	0.55	0.44	**0.93**	0.72	0.05	**0.96**	**0.92**	**0.96**
Ni													−0.06	0.45	0.03	0.67	0.19	0.30	−0.33	−0.05	0.62	−0.76	−0.40	−0.76
Zn														0.70	**0.92**	0.59	**0.95**	**0.91**	**0.92**	**0.97**	0.67	0.65	**0.91**	0.64
Cd															**0.88**	0.57	0.69	0.70	0.43	0.56	0.68	0.15	0.38	0.15
Ba																0.47	0.82	0.79	0.77	0.81	0.59	0.58	0.75	0.57
Pb																	0.82	0.88	0.38	0.67	**0.98**	−0.20	0.34	−0.20
ΣPAHs																		**0.99**	0.82	**0.97**	0.86	0.39	0.80	0.39
ΣPAHs, MW ≤ 228																			0.74	**0.93**	**0.92**	0.28	0.72	0.28
ΣPAHs, MW = 252																				**0.93**	0.41	0.82	**0.99**	0.82
ΣHopanes																					0.71	0.60	**0.92**	0.59
ΣAlkanes																						−0.13	0.38	−0.13
ΣOrganic acids																							0.85	**1.00**
ΣOA, C9–14																								0.85
ΣOA, C15–29																								

TABLE 5
DTT consumption rates (nmol/min × km) and ROS activity (μg of Zymosan units/km)

	Accord diesel	DPF-Accord	Corolla gasoline	Golf diesel	Golf biodiesel
DTT consumption*	624 ± 54	12.0 ± 1.3	29.1 ± 2.4	1300 ± 216	1040 ± 124
ROS activity	BDL	BDL	20.1 ± 1.5	17.7 ± 2.7	10.2 ± 2.4

*Data reported in Table 2, Cheung et al. (2009).

due to a combined filtering/catalytic activity. The high removal rate of PAHs confirms the effectiveness of the DPF in reducing carcinogenic compounds, which is clearly one of the major benefits of introducing this type of an after-treatment technology.

3.3. Correlations among PM Species

Table 4 presents correlations among the PM chemical species analyzed. Values with correlation coefficients >0.80 and $p < 0.05$ are in bold. Results of Cu, heavy PAHs (MW $\geq$ 276) and steranes are not included, as only 2 out of 5 data points have detectable values. Zn, P, and Ca are highly correlated ($R > 0.84$) and are all significant ingredients of lube oil. Zn and P are present in lube oil as zinc dithiophosphate, an antioxidant and anti-wear compound. The high correlations suggest that these species mostly originate from lube oil, irrespective of fuel and after-treatment technology used. The high correlations ($R > 0.88$) of these elements (Zn, P, and Ca) with hopanes further confirm this hypothesis. Furthermore, Na and K are well correlated with organic acids ($R = 0.99$ and 1.0, respectively) as they are derivatives from biodiesel.

3.4. Oxidative Potential

The DTT and macrophage-ROS assays were used to assess the oxidative potential of PM samples in this study. Table 5 shows the DTT consumption rates and ROS activity values expressed in units of distance driven. Results of DTT consumption rates were discussed in greater detail by Cheung et al. (2009) (Table 2). To summarize, the Golf vehicle produced the most potent exhaust in terms of DTT-measured oxidative activity in both configurations. The DPF-Accord vehicle reduced the distance-based oxidative potential by 98% compared to its original configuration. The gasoline vehicle was also characterized by a low DTT consumption rate due to its low mass emissions.

The macrophage-ROS assay is sensitive to transition metals because of their ability to catalyze redox-reactions in which they are not consumed. The per km-based ROS response provides the actual toxicological activity imparted on the environment and humans by these vehicles. The ROS activity, expressed in μg of Zymosan units/km, is highest for the gasoline vehicle despite its relatively low mass emissions. This is due to its higher elemental content compared to the other four configurations. The Accord vehicle, in contrast, demonstrates non-detectable ROS-measured activity in both configurations (with or without the DPF).

3.5. Correlations of PM Species with ROS and DTT

Correlations between ROS activity (μg of Zymosan units/km), DTT consumption rates [nmol/(min × km)] and selected trace elements (ng/km) were used to assess the toxicological contribution of these species to each of these assays. Results shown in Table 6 indicate that ROS is strongly correlated with

TABLE 6
Pearson correlation coefficients (R), corresponding significance levels (P), regression slopes (m) (μg of Zymosan units/ng) or [nmol/(min × ng)], and y-intercepts (b) (μg of Zymosan units/km) or [nmol/(min × km)] between ROS activity (μg of Zymosan units/km), DTT consumption rates [nmol/(min × km)], and selected elemental species (ng/km)

	Al	Ca	Fe	K	Mg	Na	P	S	V	Cr	Mn	Co	Ni	Zn	Cd	Ba	Pb	ROS
ROS																		
R	0.43	0.66	0.99	0.04	0.07	0.08	0.46	0.77	−0.07	−0.27	0.79	0.35	0.37	0.36	0.24	0.21	0.53	
P	0.47	0.23	<0.01	0.99	0.91	0.90	0.44	0.13	0.91	0.66	0.11	0.57	0.55	0.55	0.70	0.73	0.35	
m	8.36	0.13	30.2	0.00	0.22	0.01	0.28	0.06	−34.2	−20.1	11.6	133	64.6	0.32	1150	22.6	48.6	
b	7.20	3.74	−0.57	9.40	8.70	9.14	5.65	2.94	10.4	13.4	3.40	6.56	0.86	6.13	5.37	7.03	6.58	
DTT																		
R	0.72	0.83	0.36	0.44	0.82	0.56	0.92	−0.37	0.79	0.75	−0.31	0.57	0.12	0.96	0.83	0.95	0.67	0.24
P	0.17	0.08	0.56	0.46	0.09	0.33	0.03	0.54	0.11	0.15	0.61	0.31	0.85	0.01	0.08	0.01	0.22	0.69
m	859	10.5	670	1.11	152	5.24	34.8	−1.91	22631	3420	−282	13354	1299	52.2	248386	6285	3746	15.0
b	355	146	375	479	−5.0	395	112	798	69.4	-46.3	751	296	425	34.9	−310	−113	396	457.5

TABLE 7
Pearson correlation coefficients (R), corresponding significance levels (P), regression slopes (m) [nmol/(min $\times \mu$g)] or (μg of Zymosan units/μg), and y-intercepts (b) [nmol/(min $\times$ km)] or (μg of Zymosan units/km) between DTT consumption rates [nmol/(min $\times$ km)], ROS activity (μg of Zymosan units/km), and selected organic species (μg/km)

	Σ PAHs	Σ PAHs, MW ≤ 228	Σ PAHs, MW = 252	Σ Hopanes	Σ Alkanes	Σ Organic acids	Σ OA, C9–14	Σ OA, C15–29	DTT
DTT									
R	0.94	0.93	0.78	0.91	0.77	0.47	0.77	0.47	
P	0.02	0.02	0.12	0.03	0.13	0.42	0.13	0.42	
m	76.9	82.3	757	15.2	1.10	0.12	57.8	0.12	
b	142	172	228	212	311	468	231	469	
ROS									
R	0.45	0.43	0.46	0.44	0.40	0.07	0.37	0.07	0.24
P	0.45	0.46	0.44	0.46	0.51	0.91	0.55	0.91	0.69
m	0.60	0.63	7.22	0.12	0.01	0.00	0.45	0.00	0.00
b	6.03	6.33	6.04	6.53	7.16	9.27	6.73	9.28	7.21

soluble Fe ($R = 0.99$, $p < 0.01$); other elements such as S and Mn also have correlations ($R = 0.77$ and 0.79, respectively) that approach statistical significance. Valavanidis et al. (2000) measured the generation of hydroxyl radicals and indicated that oxidant generating activity is related to soluble iron ion concentrations. Since the measured ROS probe used in this method is sensitive to $HO^{\cdot}$ and H_2O_2 (Schoonen et al. 2006), the high correlation of Fe to ROS is consistent with previous findings (Valavanidis et al. 2000). Another study by Aust et al. (2002) evaluated the potential generation of ROS from vehicular PM by measuring the formation of malondialdehyde, and concluded that most ROS activity was caused by soluble iron, which is also consistent with the findings presented here (Aust et al. 2002). To a certain degree the ROS associations with other elements may be confounded by the modest association of Fe with these species, most of which are ingredients of lube oil (also shown the moderate correlation of Fe with hopanes). It is interesting, however, to note in Table 4 that other than these modest associations, Fe is not highly correlated with any other organic and inorganic species, and therefore its origin in the exhaust may be due to factors other than lube oil, such as engine wear. Ni and V are not correlated with ROS in this study, in contrast to previous studies by our group (Verma et al. 2009). This is probably due to their low emission factors (<50 ng/km for V and <7 ng/km for Ni) observed in all the vehicles tested, and consistent with the fact that Ni and V are species in urban atmospheres mostly derived from fuel oil combustion and ships (Cass and McRae 1983; Isakson et al. 2001). P, Zn, and Ba appear to have high and significant correlations with DTT. As discussed earlier, high correlations within P, Zn, and hopanes indicate that they are exclusively from lube oil. Hence, the high correlation of P and Zn with DTT might be confounders of organic species that at least mechanistically influence the DTT-measured oxidative activity.

Correlations between DTT consumption rates, ROS activity and selected organic species are shown in Table 7. Organics are the major species driving DTT, consistent with many previous studies by our group (Cho et al. 2005; Ntziachristos et al. 2007; Biswas et al. 2009a). Results of heavy PAHs (MW $\geq$ 276) and steranes are not included, as only two of the five data points have detectable values. The correlation analysis indicates that DTT rates are strongly correlated with the following species: Sum of PAHs ($R = 0.94$), lighter MW PAHs ($R = 0.93$), and hopanes ($R = 0.91$). Since heavier PAHs (MW = 252) are water insoluble, they are less correlated with DTT. The high emissions of organic acids (OA) from biodiesel do not seem to affect DTT. PAHs and hopanes have moderate correlations with ROS, but none of which reach significance. ROS and DTT are not correlated with each other due to the different development of oxidative stress in each method.

4. CONCLUSIONS

In summary, our results showed that the Golf vehicle (in both petro-diesel and biodiesel) emitted the most redox potent exhaust per km driven and also had the highest emissions of organic species (PAHs, hopanes, steranes, and organic acids). The biodiesel vehicle had elevated emissions of several organic acids due to incomplete combustion, although they did not seem to affect the oxidative properties of the emitted PM. The DPF-equipped Accord diesel car, by comparison, was effective in reducing overall PAHs and PM mass, and had the least potent emissions measured by both DTT and ROS assays. Thus, to reduce the emissions of carcinogenic aromatics, the use of advance after-treatment technologies and/or cleaner fuel may be a better remedy than the use of biodiesel. Our results indicated that soluble Fe is highly correlated with particulate ROS activity ($R = 0.99$), while PAHs and hopanes are highly correlated with the DTT consumption rates ($R = 0.94$ and 0.91, respectively). The DTT-measured PM activity was found to be strongly associated with tracers of lube oil emissions, such as Zn, P, Ca, and hopanes

(R = 0.96, 0.92, 0.83, and 0.91, respectively), suggesting that incomplete combustion of lube oil plays a significant role in the overall PM-induced toxic activity of vehicular exhaust.

REFERENCES

Andre, M. (2004). The ARTEMIS European Driving Cycles for Measuring Car Pollutant Emissions. *Sci. Total Environ.* 334–35:73–84.

Aust, A. E., Ball, J. C., Hu, A. A., Lighty, J. S., Smith, K. R., Straccia, A. M., Veranth, J. M., and Young, W. C. (2002). Particle Characteristics Responsible for Effects on Human Lung Epithelial Cells. *Research Report (Health Effects Institute)*:1–65; discussion 67–76.

Becker, S., Dailey, L. A., Soukup, J. M., Grambow, S. C., Devlin, R. B., and Huang, Y. C. T. (2005). Seasonal Variations in Air Pollution Particle-Induced Inflammatory Mediator Release and Oxidative Stress. *Environ. Health Persp.* 113:1032–1038.

Birch, M. E., and Cary, R. A. (1996). Elemental Carbon-Based Method for Monitoring Occupational Exposures to Particulate Diesel Exhaust. *Aerosol Sci. Technol.* 25:221–241.

Biswas, S., Verma, V., Schauer, J. J., Cassee, F. R., Cho, A. K., and Sioutas, C. (2009a). Oxidative Potential of Semi-Volatile and Non Volatile Particulate Matter (PM) from Heavy-Duty Vehicles Retrofitted with Emission Control Technologies. *Environ. Sci. Technol.* 43:3905–3912.

Biswas, S., Verma, V., Schauer, J. J., and Sioutas, C. (2009b). Chemical speciation of PM eMissions from Heavy-Duty Diesel Vehicles Equipped with Diesel Particulate Filter (DPF) and Selective Catalytic Reduction (SCR) Retrofits. *Atmos. Environ.* 43:1917–1925.

Cass, G. R., and McRae, G. J. (1983). Source Receptor Reconciliation of Routine Air Monitoring Data for Trace-Metals—An Emission Inventory Assisted Approach. *Environ. Sci. Technol.* 17:129–139.

Cheung, K. L., Polidori, A., Ntziachristos, L., Tzamkiozis, T., Samaras, Z., Cassee, F. R., Gerlofs, M., and Sioutas, C. (2009). Chemical Characteristics and Oxidative Potential of Particulate Matter Emissions from Gasoline, Diesel, and Biodiesel Cars. *Environ. Sci. Technol.* 43:6334–6340.

Chien, S.-M., Huang, Y.-J., Chuang, S.-C., and Yang, H.-H. (2009). Effects of Biodiesel Blending on Particulate and Polycyclic Aromatic Hydrocarbon Emissions in Nano/Ultrafine/Fine/Coarse Ranges from Diesel Engine. *Aerosol and Air Qual. Res.* 9:19–31.

Cho, A. K., Sioutas, C., Miguel, A. H., Kumagai, Y., Schmitz, D. A., Singh, M., Eiguren-Fernandez, A., and Froines, J. R. (2005). Redox Activity of Airborne Particulate Matter at Different Sites in the Los Angeles Basin. *Environ. Res.* 99:40–47.

Correa, S. M., and Arbilla, G. (2006). Aromatic Hydrocarbons Emissions in Diesel and Biodiesel Exhaust. *Atmos. Environ.* 40:6821–6826.

Donaldson, K., Stone, V., Seaton, A., and MacNee, W. (2001). Ambient Particle Inhalation and the Cardiovascular System: Potential Mechanisms. *Environ. Health Persp.* 109:523–527.

Fraser, M. P., Cass, G. R., and Simoneit, B. R. T. (1999). Particulate Organic Compounds Emitted from Motor Vehicle Exhaust and in the Urban Atmosphere. *Atmos. Environ.* 33:2715–2724.

Gauderman, W. J., Vora, H., McConnell, R., Berhane, K., Gilliland, F., Thomas, D., Lurmann, F., Avoli, E., Kunzli, N., Jerrett, M., and Peters, J. (2007). Effect of Exposure to Traffic on Lung Development from 10 to 18 Years of Age: A Cohort Study. *Lancet* 369:571–577.

Geller, M. D., Ntziachristos, L., Mamakos, A., Samaras, Z., Schmitz, D. A., Froines, J. R., and Sioutas, C. (2006). Physicochemical and Redox Characteristics of Particulate Matter (PM) Emitted from Gasoline and Diesel Passenger Cars. *Atmos. Environ.* 40:6988–7004.

Grose, M., Sakurai, H., Savstrom, J., Stolzenburg, M. R., Watts, W. F., Morgan, C. G., Murray, I. P., Twigg, M. V., Kittelson, D. B., and Mcmurry, P. H. (2006). Chemical and Physical Properties of Ultrafine Diesel Exhaust Particles Sampled Downstream of a Catalytic Trap. *Environ. Sci. Technol.* 40:5502–5507.

Harrod, K. S., Jaramillo, R. J., Berger, J. A., Gigliotti, A. P., Seilkop, S. K., and Reed, M. D. (2005). Inhaled Diesel Engine Emissions Reduce Bacterial Clearance and Exacerbate Lung Disease to Pseudomonas Aeruginosa Infection In Vivo. *Toxicol. Sci.* 83:155–165.

Hoek, G., Brunekreef, B., Goldbohm, S., Fischer, P., and van den Brandt, P. A. (2002). Association between Mortality and Indicators of Traffic-related Air Pollution in the Netherlands: A Cohort Study. *Lancet* 360:1203–1209.

Hu, S., Polidori, A., Arhami, M., Shafer, M. M., Schauer, J. J., Cho, A., and Sioutas, C. (2008). Redox Activity and Chemical Speciation of Size Fractioned PM in the Communities of the Los Angeles–Long Beach Harbor. *Atmos. Chem. Phys.* 8:6439–6451.

Isakson, J., Persson, T. A., and Lindgren, E. S. (2001). Identification and Assessment of Ship Emissions and Their Effects in the Harbour of G(o)overcircleteborg, Sweden. *Atmos. Environ.* 35:3659–3666.

Jha, S. K., Fernando, S., and To, S. D. H. (2008). Flame Temperature Analysis of Biodiesel Blends and Components. *Fuel* 87:1982–1988.

Kim, S., Jaques, P. A., Chang, M. C., Barone, T., Xiong, C., Friedlander, S. K., and Sioutas, C. (2001). Versatile Aerosol Concentration Enrichment System (VACES) for Simultaneous in vivo and in vitro Evaluation of Toxic Effects of Ultrafine, Fine and Coarse Ambient Particles—Part II: Field Evaluation. *J. Aerosol Sci.* 32:1299–1314.

Kincs, F. R. (1985). Meat Fat Formulation. *J. Am. Oil Chem. Soc.* 62:815–818.

Kittelson, D. B., Watts, W. F., Johnson, J. P., Rowntree, C., Payne, M., Goodier, S., Warrens, C., Preston, H., Zink, U., Ortiz, M., Goersmann, C., Twigg, M. V., Walker, A. P., and Caldow, R. (2006). On-Road Evaluation of Two Diesel Exhaust Aftertreatment Devices. *J. Aerosol Sci.* 37:1140–1151.

Knothe, G. (2006). Analysis of Oxidized Biodiesel by H–1–NMR and Effect of Contact Area with Air. *Eur. J. Lipid. Sci. Tech.* 108:493–500.

Landreman, A. P., Shafer, M. M., Hemming, J. C., Hannigan, M. P., and Schauer, J. J. (2008). A Macrophage-Based Method for the Assessment of the Reactive Oxygen Species (ROS) Activity of Atmospheric Particulate Matter (PM) and Application to Routine (daily–24 h) Aerosol Monitoring Studies. *Aerosol Sci. Technol.* 42:946–957.

Li, N., Sioutas, C., Cho, A., Schmitz, D., Misra, C., Sempf, J., Wang, M. Y., Oberley, T., Froines, J., and Nel, A. (2003). Ultrafine Particulate Pollutants Induce Oxidative Stress and Mitochondrial Damage. *Environ. Health. Persp.* 111:455–460.

Lloyd, A. C., and Cackette, T. A. (2001). Diesel Engines: Environmental Impact and Control. *J Air Waste Manage. Assoc.* 51:809–847.

Lough, G. C., Schauer, J. J., Park, J. S., Shafer, M. M., Deminter, J. T., and Weinstein, J. P. (2005). Emissions of Metals Associated with Motor Vehicle Roadways. *Environ. Sci. Technol.* 39:826–836.

McDonald, J. D., Reed, M. D., Campen, M. J., Barrett, E. G., Seagrave, J., and Mauderly, J. L. (2007). Health Effects of Inhaled Gasoline Engine Emissions. *Inhal. Toxicol.* 19:107–116.

Miguel, A. H., Kirchstetter, T. W., Harley, R. A., and Hering, S. V. (1998). On-Road Emissions of Particulate Polycyclic Aromatic Hydrocarbons and Black Carbon from Gasoline and Diesel Vehicles. *Environ. Sci. Technol.* 32:450–455.

Ntziachristos, L., Froines, J. R., Cho, A. K., and Sioutas, C. (2007). Relationship between Redox Activity and Chemical Speciation of Size-Fractionated Particulate Matter. *Particle and Fibre Toxicol.* 4:5.

Peters, A., Veronesi, B., Calderón-Garcidueñas, L., Gehr, P., Chen, L. C., Geiser, M., Reed, W., Rothen-Rutishauser, B., Schürch, S., and Schulz, H. (2006). Translocation and Potential Neurological Effects of Fine and Ultrafine Particles: A Critical Update. *Particle and Fibre Toxicol.* 3:13.

Pope, C. A., and Dockery, D. W. (2006). Health Effects of Fine Particulate Air Pollution: Lines that Connect. *J. Air Waste. Manage. Assoc.* 56:709–742.

Rogge, W. F., Hildemann, L. M., Mazurek, M. A., Cass, G. R., and Simoneit, B. R. T. (1993). Sources of Fine Organic Aerosol 2. Noncatalyst and Catalyst-Equipped Automobiles and Heavy-Duty Diesel Trucks. *Environ. Sci. Technol.* 27:636–651.

Sakurai, H., Park, K., McMurry, P. H., Zarling, D. D., Kittelson, D. B., and Ziemann, P. J. (2003). Size-Dependent Mixing Characteristics of Volatile and Nonvolatile Components in Diesel Exhaust Aerosols. *Environ. Sci. Technol.* 37:5487–5495.

Schoonen, M. A. A., Cohn, C. A., Roemer, E., Laffers, R., Simon, S. R., and O'Riordan, T. (2006). Mineral-Induced Formation of Reactive Oxygen Species. *Rev. Mineral and Geochem.* 64:179–221.

Seagrave, J., McDonald, J. D., Bedrick, E., Edgerton, E. S., Gigliotti, A. P., Jansen, J. J., Ke, L., Naeher, L. P., Seilkop, S. K., Zheng, M., and Mauderly, J. L. (2006). Lung Toxicity of Ambient Particulate Matter from Southeastern US Sites with Different Contributing Sources: Relationships between Composition and Effects. *Environ. Health Perspect.* 114:1387–1393.

Sheesley, R. J., Schauer, J. J., Chowdhury, Z., Cass, G. R., and Simoneit, B. R. T. (2003). Characterization of Organic Aerosols Emitted from the Combustion of Biomass Indigenous to South Asia. *J. Geophys. Res.—Atmos.* 108:D9.

Shi, X. Y., Pang, X. B., Mu, Y. J., He, H., Shuai, S. J., Wang, J. X., Chen, H., and Li, R. L. (2006). Emission Reduction Potential of Using Ethanol-Biodiesel-Diesel Fuel Blend on a Heavy-Duty Diesel Engine. *Atmos. Environ.* 40:2567–2574.

Stayner, L., Dankovic, D., Smith, R., and Steenland, K. (1998). Predicted Lung Cancer Risk Among Miners Exposed to Diesel Exhaust Particles. *Am. J. Ind. Med.* 34:207–219.

Stone, E. A., Snyder, D. C., Sheesley, R. J., Sullivan, A. P., Weber, R. J., and Schauer, J. J. (2008). Source Apportionment of Fine Organic Aerosol in Mexico City During the MILAGRO Experiment 2006. *Atmos. Chem. Phys.* 8:1249–1259.

Tsai, F. C., Apte, M. G., and Daisey, J. M. (2000). An Exploratory Analysis of the Relationship between Mortality and the Chemical Composition of Airborne Particulate Matter. *Inhal. Toxicol.* 12:121–135.

Vaaraslahti, K., Virtanen, A., Ristimaki, J., and Keskinen, J. (2004). Nucleation Mode Formation in Heavy-Duty Diesel Exhaust With and Without a Particulate Filter. *Environ. Sci. Technol.* 38:4884–4890.

Valavanidis, A., Salika, A., and Theodoropoulou, A. (2000). Generation of Hydroxyl Radicals by Urban Suspended Particulate Air Matter. The Role of Iron Ions. *Atmos. Environ.* 34:2379–2386.

Verma, V., Polidori, A., Schauer, J. J., Shafer, M. M., Cassee, F. R., and Sioutas, C. (2009). Physicochemical and Toxicological Profiles of Particulate Matter in Los Angeles during the October 2007 Southern California Wildfires. *Environ. Sci. Technol.* 43:954–960.

Vogl, G., and Elstner, E. F. (1989). Diesel Soot Particles Catalyze the Production of Oxy-Radicals. *Toxicol. Lett.* 47:17–23.

Wang, W. G., Lyons, D. W., Clark, N. N., Gautam, M., and Norton, P. M. (2000). Emissions from Nine Heavy Trucks Fueled by Diesel and Biodiesel Blend Without Engine Modification. *Environ. Sci. Technol.* 34:933–939.

Wang, Y. F., Huang, K. L., Li, C. T., Mi, H. H., Luo, J. H., and Tsai, P. J. (2003). Emissions of Fuel Metals Content from a Diesel Vehicle Engine. *Atmos. Environ.* 37:4637–4643.

Zhang, Y. X., Schauer, J. J., Shafer, M. M., Hannigan, M. P., and Dutton, S. J. (2008). Source Apportionment of In Vitro Reactive Oxygen Species Bioassay Activity from Atmospheric Particulate Matter. *Environ. Sci. Technol.* 42:7502–7509.

Zhao, Y., Bein, K. J., Wexler, A. S., Misra, C., Fine, P. M., and Sioutas, C. (2005). Field Evaluation of the Versatile Aerosol Concentration Enrichment System (VACES) Particle Concentrator Coupled to the Rapid Single-Particle Mass Spectrometer (RSMS-3). *J. Geophys. Res.—Atmos.* 110:D07S02.

Zielinska, B., Sagebiel, J., Arnott, W. P., Rogers, C. F., Kelly, K. E., Wagner, D. A., Lighty, J. S., Sarofim, A. F., and Palmer, G. (2004). Phase and Size Distribution of Polycyclic Aromatic Hydrocarbons in Diesel and Gasoline Vehicle Emissions. *Environ. Sci. Technol.* 38:2557–2567.